Transcription initiation arising from E-cadherin/CDH1 intron2: a novel protein isoform that increases gastric cancer cell invasion and angiogenesis

Hugo Pinheiro¹, Joana Carvalho^{1*}, Patrícia Oliveira^{1*}, Daniel Ferreira^{1*}, Marta Teixeira Pinto¹, Hugo Osório¹, Danilo Licastro², Renata Bordeira-Carriço¹, Peter Jordan³, Dejan Lazarevic², Remo Sanges⁴, Elia Stupka⁵, David Huntsman⁶, Raquel Seruca^{1,7}, Carla Oliveira^{1,7,#}

¹IPATIMUP-Institute of Molecular Pathology and Immunology, University of Porto, 4200-465 Porto, Portugal

²CBM S.c.r.l. Strada Statale 14 - km 163,5 AREA Science Park, 34149 Basovizza, Trieste, ITALY

³Centre of Human Genetics, National Health Institute Dr Ricardo Jorge, 1649-016 Lisbon, Portugal,

⁴Stazione Zoologica Anton Dohrn, Villa Comunale, 80121 Napoli, Italia

⁵Center for Translational Genomics and Bioinformatics, San Raffaele Scientific Institute, Via Olgettina 58, 20132 Milano, Italy

⁶British Columbia Cancer Agency (BCCA), Vancouver V5Z 4E6, Canada

⁷Faculty of Medicine, University of Porto, Porto 4200-465, Portugal

All the expression profiling data and genome binding data are available from the GEO repository.

*Equivalent contribution to the work.

#To whom correspondence should be addressed: Carla Oliveira, IPATIMUP, Rua Dr Roberto Frias S/N,

4200-465 Porto, Portugal. Phone: 00351225570700; Fax: 00351225570799, Email: carlaol@ipatimup.pt

ABSTRACT

Disruption of E-cadherin (CDH1 gene) expression, subcellular localization or function arises during initiation and progression of almost 90% of all epithelial carcinomas. Nevertheless, the mechanisms through which this occurs are largely unknown. Previous studies showed the importance of CDH1 intron 2 sequences for proper gene and protein expression, supporting these as E-cadherin cis-modulators. Through RACE and RT-PCR, we searched for transcription events arising from CDH1 intron 2 and discovered several new transcripts. One, named *CDH1a*, with high expression in spleen and absent from normal stomach, was demonstrated to be translated into a novel isoform, differing from canonical Ecadherin in its N-terminal, as determined by mass-spectrometry. Quantitative and functional assays showed that when overexpressed in an E-cadherin negative context, CDH1a replaced canonical protein interactions and functions. However, when co-expressed with canonical E-cadherin, CDH1a increased cell invasion and angiogenesis. Further, interferon-induced genes IFITM1 and IFI27 levels were increased upon CDH1a overexpression. Effects on invasion and IFITM1 and IFI27 expression were reverted upon CDH1a specific knockdown. Importantly, CDH1a was de novo expressed in gastric cancer cell lines. This study presents a new mechanism by which E-cadherin functions are impaired by cis-regulatory mechanisms possibly with the involvement of inflammatory machinery. If confirmed in other cancer models, our data encloses potential for designing targeted therapies to rescue E-cadherin function.

Keywords: E-cadherin/CDH1, isoform, gastric cancer, invasion and angiogenesis.

INTRODUCTION

E-cadherin, a protein encoded by the *CDH1* gene [ENSG00000039068] is the dominant epithelial cell adhesion molecular and plays a crucial role in epithelial tissue polarity and structural integrity (1) (2). Reduced cell-cell adhesiveness allows cancer cells to disobey their local (social) order, resulting in the destruction of histological structure; the most prominent morphological hallmark of malignant tumors (3). The most clinically relevant point in the progression of 90% or more carcinomas is believed to be mediated by disruption of normal E-cadherin expression, subcellular localization or function (4) (5). Classical gene inactivation (mutation, gene loss and promoter hypermethylation), transcriptional and post-transcriptional mechanisms (transcription repressors, RNA and protein quality control) have all been associated with E-cadherin loss and/or deregulation of its localization and function, in a wide range of epithelial tumors (6-12). Despite the strong correlation between E-cadherin loss and malignancy, the mechanism through which this occurs is not known for most sporadic and hereditary epithelial carcinomas.

Although mutations and deletions of *CDH1* remain the unique germline defects described in 47% of hereditary diffuse gastric cancer (HDGC; OMIM No. 137215) (13, 14), more than 70% of all HDGC families present germline monoallelic expression imbalance at the RNA level (10), caused by so far undetected mechanisms. The later observation is consistent with the overall E-cadherin protein expression defects found in most HDGC tumors (13) and pinpoint the key role of *CDH1* in this hereditary syndrome. The scenario in sporadic gastric cancers is somewhat similar, as approximately 90% of the cases present aberrant or absent E-cadherin protein expression and unequivocal gene inactivating mechanisms occur only in 30% of the cases (15).

While seeking for mechanisms regulating *CDH1* expression during mouse development, Stemmler and colleagues (2003 and 2005) showed that murine *CDH1* intron 2 deletions interfere with gene transcriptional activation and expression in a tissue specific manner (16, 17), strongly supporting the existence of sequences, within those regions, that may act as cis-modulators of E-cadherin expression

(18). Thus, there are unaccounted mechanisms for *CDH1* inactivation in sporadic and inherited tumors, potentially involving intronic-dependent regulation of this locus.

The specificity and complexity of gene expression patterns in cells and tissues is achieved not only by increases and decreases in expression levels of cell-specific genes, but also through alternative splicing, alternative transcription initiation, alternative polyadenylation and RNA editing (19). Recent uses of RNA sequencing (RNA-seq) have been pivotal to unveil transcript quantification, assess alternative splicing and detect novel gene structures. This overwhelming and increasing diversity on mRNA population occurs because 95-100% of all human pre-mRNAs, that contain sequences corresponding to more than one exon, are processed to yield multiple mRNAs (20, 21). Several of these new transcripts are known to regulate the canonical RNA form by many different mechanisms (22, 23). As an example, a recent paper suggests that an alternative PTK6 transcript is able to negatively regulate growth and modulate PTK6 activity, protein-protein associations and/or subcellular localization (24). To date similar findings have not been reported for *CDH1*, as no transcripts alternative to the canonical are described, besides those resulting from exon skipping events in cancerous samples. Herein, we describe transcripts arising from within *CDH1* intron 2, and address their putative role as modulators of E-cadherin expression and function in cancer cells.

RESULTS

In the present work, we intended to understand whether novel long transcripts arise from within intron 2 of *CDH1*, to characterize their expression pattern and to ascribe their putative role as modulators of E-cadherin expression, localization and function.

CDH1 locus gives rise to several transcripts in addition to the canonic

Our working hypothesis was that novel exons overlapping with annotated ESTs within intron 2 could be initiating exons of new *CDH1* transcripts. To address this, we have analyzed *CDH1* expression upstream and downstream of intron 2 in several normal human tissues by Real-time PCR and using TaqMan assays covering exon 1-2 and exon 6-7 borders. Interestingly, the expression ratio (exon 6-7)/(exon 1-2) was higher than 1 for all normal tissues analyzed suggesting increased transcription levels downstream of *CDH1* intron 2 (Fig. 1). This increased transcription was highest for peripheral blood lymphocytes (PBLs) followed by spleen, where exon 6-7 probe expression was 2-fold higher when compared to exon 1-2 levels.

The information from Public databases (UCSC Genome Browser http://genome.ucsc.edu/ and Ensembl http://www.ensembl.com) was used to retrieve the available information on the CDH1 locus. Four transcripts are currently annotated at Ensembl database for CDH1: the canonic transcript and other three transcripts either including one additional canonical exon or excluding one or three canonical exons. Importantly for the present work, none of the annotated transcripts encompass intron 2 sequences. Several overlapping expressed sequence tags (ESTs) are annotated for *CDH1* intron 2, potentially indicating that transcription from this locus could be more complex than previously anticipated (Fig. 2). As spleen was one of the tissues with higher (exon 6-7)/(exon 1-2) expression ratio, we used commercial spleen RNA to test the existence of CDH1 transcripts encompassing any of the selected ESTs, and their splicing with further downstream CDH1 exons. Among EST's tested, we identified two new exons, encoded by intron 2 sequences, each splicing with exon 3 at its canonical splice-site (Fig. 2). These two novel transcripts were called CDH1a and CDH1b (Fig. 2). Moreover, when amplifying CDH1a, we systematically verified the appearance of a higher molecular weight band that, upon sequencing, revealed to be another transcript, named CDH1j. A similar scenario was verified for CDH1b, where another splice-site was identified 10-bp upstream of the one initially recognized. This variant was coined CDH1b-10 (Fig. 2). All four new transcripts were found to splice with the canonical exon 3 splice-site and to include all

downstream *CDH1* canonical exons (Fig. 2), as determined by primer-walking PCR (data not shown). Additionally, only *CDH1a* and *CDH1b-10* were found to have in-frame initiation codons (AUG). *CDH1a* presents a competent Kozak sequence upstream of the AUG (data not shown) in contrast to the one from *CDH1b-10*. We have also assessed the polyadenylation status of these transcripts and inquired about the DNA strand from which they were derived. *CDH1a* and *CDH1j* were found to be polyadenylated contrarily to *CDH1b* and *CDH1b-10* (data not shown). All were found to arise from the sense strand.

In order to determine the transcription start site (TSS) of novel *CDH1* transcripts, we used spleen and stomach 5' RACE-ready cDNA libraries (built from polyadenylated RNA). These tissues were chosen for this purpose because spleen, as a non-epithelial tissue, is described to lack canonical E-cadherin expression and presented a high (exon 6-7)/(exon 1-2) *CDH1* expression ratio, indicating the presence of additional transcripts. Differently, in stomach, an epithelial tissue, E-cadherin canonical expression is well recognized and was shown to have a low (exon 6-7)/(exon 1-2) expression ratio (Fig. 1). Using this strategy, we observed that, in spleen, *CDH1a* and *CDH1j* represented more than half of the total polyadenylated RNA molecules amplified. Additionally, we observed the existence of two additional transcripts, one starting in intron 1 (*CDH1Seq1*) and other in exon 3 (*CDH1Seq5*, that probably corresponds to the Ensembl annotated transcript was not detected in spleen (Fig. 2). For stomach, the canonical *CDH1* ranscript was not detected in spleen (Fig. 2). For stomach, the canonical transcript was the main RNA form found (45%), although transcripts starting in intron 1 (*CDH1Seq11-13*), similar to those identified in spleen, were also identified in stomach, the remaining *CDH1a*, *CDH1j*, *CDH1b* and *CDH1b-10* were not found (Fig. 2 and Supplementary Figure 1).

For *CDH1a*, two 5'-sequences upstream of the same in-frame AUG were recurrently identified (*CDH1Seq2* and *CDH1Seq3* in Fig. 2) and therefore assumed as two different TSSs. The presence of these was further confirmed when its sequence was compared with CAGE data extracted from the Encode Project database at UCSC genome browser (http://genome.ucsc.edu/). For *CDH1j* transcript, the right

location of potential TSSs was harder to infer, due to high variation in the length of sequences obtained by 5'RACE. This transcript is most probably a non-coding RNA, due to lack of identifiable AUG with a long open-reading frame and Kozak sequence. *CDH1b* and *CDH1b-10* transcripts, shown earlier to be non-polyadenylated, were not found in this 5'-RACE experiment (Fig. 2).

The sequence of novel CDH1 exons overlaps or is in close vicinity of genomic regulatory features and conserved non-coding sequences.

Approximately 15% of all *CDH1* transcripts in spleen and 60% in stomach start within or upstream of *CDH1* intron 1. These transcripts, together with *CDH1Seq10* from stomach (Fig. 2), overlap a CpG island that is well known to modulate the expression of the canonical transcript as first described by Berx et al (1995) (2). Thus, similarly to the canonical transcript, the expression of these novel transcripts may also be influenced by methylation at this CpG island. Additionally, a First Exon (EF) element is predicted to overlap the initial exon of the canonical transcript (exclusive of stomach), and the novel exon encoded by a portion of intron 1 belonging to a transcript that is present in both tissues studied (Fig. 2). The presence of this element and its proximity to the latter novel exon encoded by intron 1 (*CDH1Seq1*), indicates that this exon is likely the first exon of a novel *CDH1* transcript.

Several DNAse I hypersensitive sites, which are commonly associated with new areas of transcription and/or gene regulation, were annotated in the vicinity of *CDH1a* and *CDH1b* sequences (25) (Fig. 2). Moreover, an AluSc repeat was found to overlap the sequence of the longer form of *CDH1a* that encodes the *CDH1j* transcript, likely indicating an Alu-mediated exonization event (26) (Fig. 2).

At the beginning of the canonical exon 3, a predicted CCCTC-binding factor (CTCF) binding site was also found, what may be important to explain the percentage of RNA transcripts starting immediately downstream of this site in stomach (~40%) and in spleen (~15%) (Fig. 2).

Fig. 2 was constructed based both on several tracks of UCSC and the Ensembl Genome Browser and our own data and depicts in detail the data described above.

We also investigated the extent of mammalian sequence conservation for the *CDH1a* and *CDH1j* transcripts identified. We verified the nucleotide level GERP score (27) for each transcript, focusing only on the novel portion (i.e. the part of the transcript that had not been previously reported). As shown in Supplementary File 1, *CDH1a* transcripts appear to be evolutionarily constrained, with mammalian sequence conservation across most of their sequence in line with that of UTR portions of genes (median GERP score 1.72, max GERP score=3.67 for both the longer *CDH1a_70* transcript and shorter *CDH1a_34 transcript*). *CDH1j*, on the other hand, shows a very different conservation pattern. The median GERP score indicates that there is no long-range evolutionary constraint across the transcript, but the sliding window analysis indicates clearly that the final portion of the *CDH1j* exon is highly conserved (nt 320-352), which has a median GERP score of 2.3. Interestingly the highly conserved portion also corresponds to the DNAase I hypersensitivity site.

CDH1a expression is tissue-specific

We characterized *CDH1a* in detail as, unlike the other *CDH1* novel transcripts, it has cumulatively a polyadenylated open-reading frame encoding a novel 5'-exon transcribed from within intron 2, encompasses two possible TSSs, an adequate Kozak consensus sequence upstream of the AUG, and splices with the canonical exon 3, sharing all downstream exons with the *CDH1* canonical transcript. This RNA transcript encloses most of the necessary features to be translated into a protein isoform and is also particularly interesting because it is the most abundant *CDH1* transcript in spleen (~50%) and is completely absent in stomach, according to the 5'-RACE results.

Using PCR followed by Q-SnapShot (10), we addressed *CDH1a* pattern of expression in several normal tissues. We have confirmed high *CDH1a* expression for spleen and its absence in stomach (Fig. 3A),

contrasting with the scenario obtained for *CDH1* canonical transcript (Fig. 2). Although highest *CDH1a* expression levels have been found for spleen, other normal tissues displayed variable expression of the transcript. Interestingly, the expression of *CDH1a* in PBLs was not comparable to that observed when measuring the (exon 6-7)/(exon 1-2) expression ratio depicted in Fig. 1 which indicates that this is likely due to the expression of other transcripts starting downstream of exon 2 in PBLs.

Given that *CDH1a* mRNA levels were high for spleen, no canonical transcript was present and no other open-reading frames were identified by 5'-RACE, we reasoned that if a protein isoform was being produced from this transcript, it would be caught by immunohistochemistry using an antibody against any portion of the canonical protein, encoded by exons downstream of exon 3. For that, we stained both normal human spleen and stomach sections with an E-cadherin antibody that recognizes the protein (E-cadherin and putative CDH1a isoform) cytoplasmic domain. In spleen, we observed a very specific and localized staining pattern (Fig. 3B), in contrast to the typical staining of the canonical E-cadherin at the basolateral surface of adjacent cells in gastric glands (Fig. 3C). Although fairly similar to small blood vessels in aspect, the stained structures observed in spleen showed no co-localization with CD34, a marker of endothelial cells (Suppl. Fig. 1). Together, these observations support that *CDH1a* is translated and encodes a novel E-cadherin isoform in spleen.

Exogenous overexpression of CDH1a generates a protein that is less efficiently processed to a mature form than canonical E-cadherin

In order to assess CDH1a protein isoform translation and potential processing, we cloned the full transcript sequence from the AUG to the stop codon in a Lentiviral derived expression vector (pLenti, Invitrogen). Empty vector (Mock) and the vector carrying canonical *CDH1* cDNA (*E-cadherin*) were also generated as negative and positive controls, respectively. The Chinese Hamster Ovary (CHO) cell line was chosen to be transduced due to its complete lack of E-cadherin expression. The predicted aminoacidic

differences between E-cadherin and CDH1a sequences are depicted in figure 4A. The canonic sequence **Met**GPWSRSLSAL...RHLERGRVLGR transcribed from the exon 1 and 2 sequences is replaced by **Met**KLKLSRKQIQHGDKAAAVSLL, the aminoacids encoded by the new exon 1a. Through western blot and using an antibody capable of detecting both the canonical and also CDH1a isoforms (Fig. 4A), we were able to prove the effectiveness of transduction and to confirm that, upon lentiviral promoter influence, *CDH1a* is efficiently translated into a protein of approximated size to that of the canonical E-cadherin (Fig. 4B). As expected, the empty vector (Mock) cells did not induce E-cadherin expression.

Since the immature form of E-cadherin is predictably processed to its mature form by cleavage of the 154 aminoacid residues precursor sequence, we analyzed whether CDH1a isoform would be cleaved in a similar way. Using brefeldin A, that blocks the transfer of the protein to the Golgi complex and its processing (28), we verified for both (CDH1a isoform and E-cadherin), bands corresponding to the mature proteins displayed comparable molecular weight, whereas the immature proteins did not. This result confirms that CDH1a pre-protein is smaller than the canonical E-cadherin and further that the two proteins are cleaved, if not at the same site, in very close proximity (Fig. 4C).

To confirm the relative amount of mature and immature proteins between cells expressing the canonical or the CDH1a protein isoform, we proceeded to protein sequencing by mass spectrometry using bands extracted from the gel (Fig. 4E). Protein lysates were immunoprecipitated using an anti-E-cadherin antibody and the resulting eluate was separated by 1D SDS-PAGE from both CHO E-cadherin and CHO CDH1a expressing cell lines. For each cell line two bands with different molecular weights were observed, possibly related with E-cadherin immature (higher molecular weight) and mature (lower molecular weight) forms as seen in Fig. 4C. For CHO E-cadherin, both bands were identified by MALDI-TOF/TOF mass spectrometry as E-cadherin with a C.I. of 100% (Supplementary Table 2). Thirty peptides were found to be associated to E-cadherin (UniProt accession ID P12830) from CHO E-cadherin, both in higher and lower molecular weight mass.

CDH1a bands also presented 19 peptides associated with E-cadherin (Uniprot accession ID P12830) that were common to the canonical E-cadherin. In addition, an extra peak was identified with a mass of 1722.85Da, that was absent for CHO E-cadherin (Suppl. Fig. 2). To verify that this novel peak was associated with CDH1a N-terminus, we downloaded the Swiss-Prot/UniProt protein sequence database and manually inserted the full CDH1a sequence. A Mascot Peptide Mass FingerPrint (PMF) analysis successfully associated this 1722.85Da peak as well as identified a smaller one with 953.52Da with CDH1a sequence, corresponding, respectively, to the N-terminal peptides AAAVSLLVNFEDC*TGR 16-31 (C*, carbamidomethylation of cysteine) and KQIQHGDK 8-15 (Supplementary Table 2). To further validate this result, the 1722.85Da peak, which presented the best signal to noise ratio, was subjected to MS/MS peptide sequencing followed by a PMF+MS/MS combined analysis. A Mascot ion score of 99.9% was obtained for this peptide (Supplementary Table 2). Peptide sequencing was not possible for the smaller peak (953.52Da), nevertheless its presence is consistent in the two bands analyzed and specific from CDH1a expressing cells (two independent replicas).

It is also worth noting that, for the lower molecular weight E-cadherin band, presumably indicating the mature form (Fig. 4E), the combination of the first 3 N-terminal peptides (aa 55 to 74), observed after tryptic digestion, are decreased 8.8-fold in E-cadherin and the first 4 N-terminal peptides (aa 8 to 42) decrease 3.5-fold in CDH1a when compared with all the other peptides (Supplementary Table 2). This indicates that CDH1a processing is 2.5 (8.8/3.5) times less efficient than E-cadherin processing. In the immature E-cadherin and CDH1a higher molecular weight bands, the intensity of the peptide peaks associated with the protein's N-terminal does not significantly change, when compared with the peptide peaks associated with other regions of E-cadherin, as expected when the processing is efficient.

The results obtained for both E-cadherin isoforms confirm their identity and reveal that CDH1a is less efficiently processed to a mature form than canonical E-cadherin, but are not sufficient to determine the potential sites of cleavage for each isoform. They show, nevertheless, that *CDH1* and *CDH1a* encode two

distinct proteins with different N-terminal regions that, independently of the processing, exist in the cell with potentially different functions.

CDH1a isoform mimics canonical E-cadherin localization, adhesion complex interactions, celladhesion and invasion suppression properties when overexpressed in canonical E-cadherin-negative cells

To assess CDH1a function, we conducted immunoprecipitation in protein extracts from cells expressing CDH1a (and the canonical form, for positive control) using the same anti-E-cadherin antibody, followed by western blot for proteins that classically interact with E-cadherin to form the adhesion complex (β -catenin and p120ctn). Our results demonstrate the effective binding of both proteins to these catenins (Fig. 4D) and are further supported by immunofluorescence results showing that CDH1a is able to induce β -catenin (Fig. 4E) and p120-catenin (Fig. 4F) recruitment to the cell membrane. This argues towards the putative functionality of CDH1a protein in establishing an effective adhesion complex. Moreover, we observed that CDH1a, similarly to E-cadherin, was able to confer aggregation capacity to the otherwise non-aggregating CHO cells (Fig. 4G) and to reduce the intrinsic invasion levels of parental CHO cells (Fig. 4H). Overall, these results show that CDH1a isoform, when expressed alone, mimics the canonical E-cadherin function.

CDH1a promotes cell invasion and angiogenesis when co-expressed with the canonical E-cadherin

We next addressed the CDH1a induced expression effect in cells endogenously producing functional Ecadherin. For that, we chose the gastric cancer derived cell line MKN28. Due to suboptimal proportion of MKN28 *CDH1a* expressing cells, using the pLenti vector, we subcloned *CDH1a* and the canonical *CDH1* into a pIRES2-EGFP vector that expresses our protein of interest and GFP in the same cell. This approach allowed sorting GFP positive cells and monitoring transfection efficiency which reached around 90% (Fig. 5A and B). Overexpression from either the canonical E-cadherin or *CDH1a* has not produced visible alterations in the overall E-cadherin expression levels or cellular localization, as ascertained by immunocytochemistry (Fig. 5C).

We confirmed mRNA overexpression of the canonical *CDH1* or *CDH1a* using the previously described strategy, where exon 1-2 probe expression measures specifically canonic transcript expression and exon 6-7 expression measures overexpression of both transcripts. As expected, an increase in canonic *CDH1* mRNA expression was detected by both probes, for cells transfected with the canonical *CDH1* expression vector in comparison to Mock cells; whereas an increase in *CDH1a* mRNA overexpression was detected only by the Exon 6-7 probe (Fig. 5D).

Surprisingly, the results obtained by western blot did not mimic the previous RNA expression data, since similar levels of E-cadherin protein were detected for the three cell lines (Fig. 5E). To unveil whether the excess of translated protein, due to the forced production of high levels of mRNA from both isoforms, was being degraded, we treated the three cell lines with MG132, a proteasome function inhibitor. We confirmed that this was the case, as significantly increased protein levels were detected both in E-cadherin and *CDH1a* overexpressing cells (P=.001 and P=.020, respectively) in contrast to Mock cells, after the treatment with this drug (Fig. 5F).

Assuming that the proteasome blindly degrades both isoforms in CDH1a overexpressing cells, a proportion of the detected protein by western blot and immunohistochemistry is expected to be the CDH1a isoform. Moreover, in CDH1a overexpressing MKN28 cells, high amounts of unprocessed CDH1a seem to occur, as shown by the abnormal superior thickening of the western blot signal (Figure 5F). In contrast to canonical CDH1 overexpressing MKN28 cells, separation between the upper and the main lower band (presumably the mature processed form) is not clear, due to the smaller difference between the unprocessed and processed proteins when compared to the canonical form.

To prove this, we have repeated mass spectrometry analysis and showed that the CDH1a specific peaks (953.52Da and 1722.85Da) are found in MKN28 CDH1a overexpressing cells (Supplementary Table 3 and 4).

Next, we carried out aggregation, motility and invasion experiments to access the effect of concomitant expression of the two isoforms. We verified that CDH1a overexpression increased cell aggregation capacity in comparison with Mock cells, nevertheless this augmented aggregation ability was lower than that induced by the canonic isoform (Fig. 6A). No differences were found in motility levels for the three cell lines (data not shown), which contrasted with results obtained for the invasion assay. CDH1a overexpression in MKN28 cells led to a significant increase in the number of invasive cells when compared to cells overexpressing E-cadherin or the empty vector (Fig. 6B). Taken together, these data indicates that CDH1a overexpression induced less efficient cell aggregation, did not affect cell motility but conferred an invasive phenotype to otherwise poorly invasive cells. No differences were observed in the three cell lines regarding cell proliferation or apoptosis (data not shown).

We further tested the effect of *CDH1a* overexpression in MKN28 cells regarding tumor induced angiogenesis, using the classical chick embryo chorioallantoic membrane (CAM) *in vivo* model (29-31). The angiogenic response levels were quantified by counting the number of novel radial blood vessels formed in tumors induced by every cell line, and verified that tumors formed by CDH1a overexpressing cells were the ones eliciting significantly more blood vessels when compared with cells transfected with the empty vector (Fig. 6C and D). By pan-cytokeratin immunoexpression, we confirmed that tumors growing in the CAM were exclusively formed by the human cells (Fig. 6E) and demonstrated by PCR that these maintain *CDH1* and *CDH1a* overexpression patterns (Suppl. Fig. 3).

CDH1a overexpression in MKN28 cells increases IFITM1 and IFI27 mRNA levels

In order to determine the effect of CDH1a overexpression on the overall mRNA expression pattern of pLenti transduced MKN28 cells, we performed a genome-wide mRNA expression array analysis. This experiment identified 50 genes (76 probes) whose expression was upregulated and 33 genes (42 probes) whose expression was downregulated (Suppl. Fig. 4 and Suppl. File 3). In Supplementary Table 5, we have presented the 24 most altered (positively or negatively) genes, from which we selected preferentially upregulated genes for qRT-PCR validation. The eight genes with top fold-change and lower *P*-values were tested as well as two of the top downregulated genes. We were able to confirm IFN-induced transmembrane protein 1 (IFITM1) and IFI27 overexpression by qRT-PCR, specifically in cells overexpressing CDH1a (Fig. 7A and B) while for the other genes no consistent results were found (Suppl. Fig. 5). IFITM1 levels were also upregulated upon CDH1a overexpression in HEK cells (data not shown).

We performed Ingenuity analysis on the list of significant differentially expressed genes to select the functional classes (defined as network) overrepresented. The highest Ingenuity scoring networks contain the most statistically robust candidates for hypothesis building. Inflammatory response result to be the most significant network in our analysis (Suppl. Fig. 6, see also Suppl. File 3). Interestingly, 4 out of 15 genes of the network known to be involved in gastric cancer are present in the list of differentially expressed. The other significant networks overrepresented in CDH1a responsive genes are cellular growth and proliferation, cellular movement, cancer and cell death (Suppl. file 2). Through a PGSEA analysis, the TGF- β pathway was predicted to be upregulated in MKN28 CDH1a cells when compared to controls (Suppl. Fig. 7).

16

Invasion levels are restored and IFITM1 and IFI27 are lowered upon siRNA-mediated CDH1a downregulation

In order to definitively demonstrate that the observed increases in invasion, and *IFITM1* and *IFI27* expression levels are driven by CDH1a overexpression, we designed a specific siRNA to target specifically this transcript. A 35% reduction in *CDH1a* levels (Fig. 8A) was sufficient to lower significantly invasion levels by 73% (Fig. 8B) and *IFITM1* and *IFI27* by 31% and 45%, respectively. Canonical *CDH1* expression displayed no alteration (Fig. 8C).

CDH1a transcript is overexpressed in gastric cancer cell lines

Having observed the CDH1a potentially deleterious effects over canonical E-cadherin function, and given that *CDH1a* mRNA was not expressed in normal stomach, we tested its expression in gastric cancer derived cell lines along with canonical E-cadherin expression. Interestingly, we observed an inverse correlation between *CDH1a* and canonical *CDH1* mRNA expression in normal stomach and gastric cancer cell lines (Fig. 9A and B). While the canonical form was highly expressed in normal stomach and presented an overall downregulation in gastric cancer cell lines, *CDH1a* mRNA was absent in normal stomach, as previously observed, and overexpressed in most gastric cancer cell lines (Fig. 9A and B). Moreover, most gastric cancer cell lines were found to co-express the canonical *CDH1* and *CDH1a* mRNAs.

DISCUSSION

Loss of the epithelial adhesion molecule E-cadherin is thought to be the earliest and one of the most important steps in metastatic dissemination of epithelial cancer (7, 32). Although impairment of E-cadherin gene and protein expression has been the subject of many studies, the causes for this disruption are, in many cases, unknown and the mechanisms so far described insufficient. It is possible that driver events for this impairment could be embedded in the genomic structure of the *CDH1* gene itself. The pioneer studies by Stemmer and colleagues (16, 17) showed that regulation at the *CDH1* locus can be driven by powerful yet unidentified regulatory sequences with the 65kb intron 2 of this gene. In the present study, we studied novel and conserved coding intron 2 sequences, and described the tissue specificity and potential biological function of one of them.

This is, to the best of our knowledge, the first report specifically addressing *CDH1* alternative transcription, besides the alternative splicing variants, involving canonical exons, deposited in public databases. After proving that the mRNA sequences downstream of intron 2 were more represented in several normal tissues than those upstream of this intron, we tested whether annotated Expressed Sequence Tags (ESTs) within *CDH1* intron 2 could be transcribed into novel *CDH1* exons. Two of these ESTs were shown to encompass novel exons able to splice with exon 3, sharing the remaining exons and termination with the canonic sequence. Both exons are targets of alternative splicing and each new exon generates at least one in-frame transcript and one long-noncoding RNA. This finding reveals the existence of novel E-cadherin transcripts in normal contexts. Somewhat surprisingly, spleen, that was shown not to express canonical transcript, expresses high levels of CDH1a, a novel protein encoding transcript that localizes at the cell membrane of structures from the splenic red medulla.

We were further able to map important genomic elements overlapping or near the novel transcription units herein described, such as a CpG island, Dnase I hypersensitive sites and a CTCF binding site, that re-enforce their significance and potential function (Fig. 2). CpG islands are regions commonly found near transcription start sites and frequently associated with promoter regions. This fact constitutes evidence towards the possible regulation of novel transcripts through promoter methylation, as happens for the canonic CDH1 transcript. Dnase I hypersensitive sites, uncovered by ChIP-Seq experiments (UCSC Genome Browser tracks) tend to be near active genes, which are regularly transcribed (25). At the beginning of CDH1 exon 3 a predicted CCCTC-binding factor (CTCF) is found (UCSC Genome Browser tracks), which characteristic insulator function (33, 34) may justify the low percentage of RNAs starting after this region in stomach. Here, as an epithelial tissue, E-cadherin is known to exert well-established functions and must be, therefore, tightly regulated. This would allow preventing putative deleterious effects from the concomitant expression of other transcripts from the CDH1 locus. In contrast, for spleen, as non-epithelial tissue, CDH1 locus may somehow be more loosely controlled originating a broader variety of coding and noncoding transcripts of thus far uncertain functional relevance. Interestingly, one of the noncoding transcripts (CDH1i, depicted as Seq4 in Fig. 2B) was found to encompass an AluSc repeat. The Alu family is composed of over one million repetitive elements of about 300 base pairs long that are interspersed throughout the human genome and embrace more than 10% of it (9, 35). Alu repeats have been implicated in the etiology of rearrangement based deleterious mutations reported of CDH1 and other genes (9). In addition, such transposable elements have been shown to cause alternative splicing by providing the 5' or 3' splicing sites in so-called "exonization events" (36). Other regulatory mechanisms also involving Alu elements have been recently reviewed (37).

Overall evidence indicated that while *CDH1a* is a bona fide novel protein coding transcript while the other transcripts identified are more likely to play a role at non-coding level. The conservation analysis underlined this difference, since *CDH1a* showed constant overall conservation, while *CDH1j* showed a conservation pattern which is more typical of enhancer like elements, with short blocks of high conservation. Transcribed enhancers have been shown to exist extensively, especially across highly conserved elements (38), thus it is possible that *CDH1j* is a transcribed enhancer.

We further characterized one of the novel transcripts, CDH1a, selected because it possesses a long ORF, an adequate Kozak sequence, is polyadenylated and is therefore predicted to encode a novel E-cadherin protein isoform. We then determined that CDH1a, an isoform that differs from the canonical one only at the most N-terminal residues, which were predicted to be cleaved from the mature form of the protein, could work as a negative modulator of the canonical E-cadherin function. This kind of effect has been previously described (23).

We were able to show that CDH1a isoform, driven by a pLenti vector, gave rise to a mature protein similar in size to the canonic. As expected, the size of the immature form was found to be smaller since canonic exons 1 and 2 are replaced by a new exon (exon 1a) in *CDH1a*. CDH1a was able to replace the canonical protein function, in that its protein location at the membrane, partner interactions co-localizing with β -catenin and p120-ctn, aggregation induction and invasion suppression properties when expressed on its own match those of canonical E-cadherin. These data imply that, in the absence of the canonic E-cadherin, its functions may be accomplished by the new isoform herein described. Nevertheless, there are differences between E-cadherin and CDH1a, as two N-terminal specific peptides from the latter (953.52Da and 1722.85Da) were detectable by mass spectrometry in CDH1a expressing cells. These peptides potentially constitute good targets for antibody design to better disclose CDH1a expression pattern.

Interestingly, the behavior induced by CDH1a expression alone, was not mimicked when CDH1a was expressed in a context of endogenous canonical E-cadherin expression. In this setting, canonic protein localization was not impacted to a perceivable extent, but CDH1a forced expression led to moderate aggregation impairment and significantly increased angiogenic potential and invasion levels. Invasion increase was reverted upon *CDH1a* targeting through specific siRNA. A similar observation has been recently described in breast cancer derived cell lines (39). These authors showed that co-expression of P-cadherin and canonical E-cadherin in MCF7 cells promoted invasion *in vitro*, while their counterparts expressing either molecule alone would remain non-invasive. The effect of CDH1a may be comparable in

that CDH1a overexpression hampers E-cadherin normal function despite the cells epithelial phenotype is maintained. When we overexpressed CDH1a in E-cadherin expressing cells no increase in protein levels was observed unless we treated cells with a proteasome inhibitor. This led to a significant augment in total protein levels, implying that total protein levels are controlled by the ubiquitin-proteasome machinery (40, 41), over a given expression threshold. We therefore hypothesize that the observed consequences at the functional level in cells co-expressing CDH1a and the canonical form, can only occur if the cell blindly degrades both isoforms and not only CDH1a. The co-existence of both molecules, despite their similarities and expression at the right amounts, provides cancer cells with an advantageous invasive phenotype. The means by which this phenotype is achieved is not known, although our experiments indicate that CDH1a is less efficiently processed than E-cadherin. It is possible that the extra peptides in the mature CDH1a determine the effects observed either directly or indirectly through a number of genes with altered expression levels, upon CDH1a overexpression, as revealed by our expression microarray analysis. This experiment identified 50 upregulated genes and 33 downregulated. We performed Ingenuity analysis on the list of significant differentially expressed genes to select the functional classes (defined as network) overrepresented. The highest Ingenuity scoring networks containing the most statistically robust candidates for hypothesis building indicated the Antimicrobial Response, Inflammatory Response and Infectious Disease network as the most significant, despite others have also putatively interesting results. Importantly 4 out of 15 genes from the network known to be involved in gastric cancer are present in the list of differentially expressed. Since our previous results were indicative of gain of function effects, we gave greater importance to upregulated genes. We have therefore selected the eight genes with higher fold-change and lower P-values, when comparing MKN28 CDH1a overexpressing cells with controls, for qRT-PCR validation. We have selected also two downregulated genes. Possibly due to the different vectors used to establish cells for the array experiment and qRT-PCR validation we had a low level of concordance between both techniques. This, however, strengthens the results obtained for IFITM1 and IF127 genes. These were the only genes with

upregulation validated by qRT-PCR (besides *CDH1*) and interestingly they are part of the above referred network. *CDH1a* siRNA treatment led to the downregulation of both *IFITM1* and *IFI27*.

IFITM1 is a member of the IFN-inducible transmembrane protein family and its involvement in the migratory and invasive potential of gastric cancer cells is well established, supporting our data (42). It was established that IFITM1 induces tumor resistance to NK cells in gastric tumor cells, being hypothesized that it behaves like a surface molecule utilized by tumor cells for immune escape and migration, making of IFITM1 a possible therapeutic target for the treatment of gastric cancer. Recently, IFITM1 was implicated in the invasive front of early invasive and advanced HNSCC (43, 44) and its knockdown has been shown to significantly inhibit migration and invasion of glioma cells (44).

IFI27 was identified in breast carcinoma cell lines (45) and belongs to a family of small, interferon-alpha (IFN- α)-inducible genes. Suomela S *et al* proposed IFI27 as a novel marker of epithelial proliferation and cancer due to its upregulation in cutaneous squamous cell cancers (46) as confirmed later (47).

A Parametric Gene Set Enrichment Analysis (PGSEA), that allows the analysis of gene expression data to determine deregulation of gene signatures or "molecular concepts", suggested that CDH1a overexpression in canonical E-cadherin expressing cells could impact the TGF-β pathway.

We observed that when compared to control cell lines, CDH1a overexpressing cells have upregulation of the transforming growth factor- β (TGF- β) pathway, which has a well-recognized dual role both in tumor initiation and progression (48) and in tumor suppression (49, 50). The mechanisms of tumor promotion by TGF- β include increased angiogenesis. The impact of CDH1a overexpression on the latter was seen through a marked increase in angiogenesis in the chick embryo chorioallantoic membrane (CAM) model. It is therefore possible that this induction of angiogenesis is triggered by TGF- β pathway upregulation, although the mechanism through which this pathway is activated remained elusive after the expression array performed. Other pathways enclosed by the networks revealed by the Ingenuity analysis might, as well, be implicated in this angiogenic effect of CDH1a.

Since stomach was the only normal tissue in this study lacking endogenous CDH1a expression, we decided to search for its *de novo* expression in gastric cancer derived cell lines. Interestingly, and in contrast to what was observed for normal stomach, most expressed CDH1a. This indicates that transcription arising from CDH1 locus may be deregulated in the gastric cancer context, resulting in the co-expression of both the canonic transcript and CDH1a, possibly leading to the deleterious effects mentioned above (Fig. 10). Despite many efforts, we were not able to identify CDH1a isoform endogenous expression in MKN28 nor in other gastric cancer cell lines. The reason for this inability may be explained by a recent report that has shown that proteins with deleterious effects when overexpressed have lower abundances than the normal protein due to shorter half-lives (51). Additionally these proteins are predicted to display higher structural disorder (52, 53) and the severity of deleterious phenotype is strongly associated with percent of disorder (51). In a cancer context, the ability of a cell to control the relative amounts of proteins with deleterious functions is predictably reduced and therefore negative consequences are more prone to arise. The way a protein is deleterious is not unique. A protein may carry specific domains that by themselves, or through their interactions, are toxic. Other proteins show high intrinsic disorder, which is likely to be associated with their deleterious effect. Yet others are tightly regulated, and are likely to perturb cellular homeostasis when the dynamics of their expression is disrupted. At the moment we cannot put forward which applies for CDH1a although our results seem to favor the last hypothesis.

In summary, our work describes, for the first time, tissue-specific coding and noncoding *CDH1* transcripts arising from new exons encoded by intron 2 sequences, and highlights a possible novel mechanism underlying epithelial cancer cell invasion and angiogenesis. It is possible that the unique CDH1a peptides described and the potential effectors IFITM1 and IFI27 could become therapeutic targets and that isoform-specific antibodies could be designed to target CDH1a-mediated cancer invasion and angiogenesis.

MATERIALS AND METHODS

Biological samples and cell lines

In order to perform transcripts quantification we have purchased commercial total RNA from several normal tissues: spleen (Ambion), stomach (Ambion), colon (Stratagene) and breast (Stratagene). Regarding thyroid and peripheral blood lymphocytes (PBLs) we have pooled several samples from normal controls available at IPATIMUP. We have quantified CDH1a and the canonical transcript in RNA samples from MKN28, MKN45, GP202, SNU1, SNU638, KATOIII, AGS, IPA220 and NCI-N87 gastric cancer cell lines, available at the IPATIMUP's repository. The cell lines used for transduction and transfection experiments were: 1) the Chinese Hamster Ovary (CHO) cell line, as a cadherin-free cell line, and; 2) the human gastric cancer derived MKN28, as a model with normal and functional E-cadherin. Normal stomach and spleen tissues used for immunohistochemistry were obtained from paraffin blocks from the Hospital S.João tissue bank (Porto, Portugal) and VU University Medical Center (Amsterdam, The Netherlands). Chicken fertilized eggs for the angiogenesis assay were acquired from commercial sources (Granja Santa Isabel, Spain).

Bioinformatics

Using the Ensembl database (http://www.ensembl.org, version 64, September 2011 (54) and the UCSC Genome Browser (http://genome.ucsc.edu, NCBI36/hg18 (50) we have collected data on several genomic elements predicted/annotated within *CDH1*'s intron 2 genomic locus: 1) *CpG* islands (49, 54); 2) *EF* (First Exon Finder) elements (54, 55); 3) *Alu* repeat elements (54, 56); 4) *CTCF* (CCCTC-binding factor) sites (34, 54); 5) DNAse I Hypersensitive Sites (49, 56); 6) *EST* (Expression Sequence Tags) from the database *dbEST* (*54, 57*) and; 7) *CAGE* (Cap Analysis Gene Expression) tags from the ENCODE project (58, 59). CAGE data collected refers to those obtained using the "normal" lymphoblastoid cell line *GM12878* and the leukaemia cell line *K562*. RNA populations analysed include total RNA and polyA

negative RNA. Subcellular compartments analysed include nucleus, cytosol, nucleoplasm, polysome and chromatin (60).

Using the annotated Expression Sequence Tags (EST) present in the UCSC Genome Browser (http://genome.ucsc.edu/cgi-bin/hgTracks), we have designed primers to amplify specifically new areas of transcription.

To assess *CDH1a* and *CDH1j* sequence conservation, the nucleotide level GERP score (27) was downloaded from the UCSC genome browser, using the start and end coordinates of the novel portion of the transcript identified (i.e. excluding the known protein-coding portion of CDH1), as shown in Supplementary File 1. The data was then assessed both at the single nucleotide level (first column in the table), as well as using a 10bp sliding window (second column in the table and shown also as graph). Overall conservation was indicated by verifying the average, median, minimum and max GERP score observed across the entire region. Local conservation for *CDH1j* was investigated by searching for blocks which presented more than 10nt with GERP score >1, highlighted in yellow in the table. The table also contains a UCSC screenshot showing GERP score, transcription score based on ENCODE RNA-Seq data, and ENCODE DNAase I hypersensitivity regions.

RNA isolation and cDNA synthesis

RNA Isolation was performed using the Tripure Isolation Reagent (Roche). RNA quality was verified using the NanoDrop ND-1000 (Thermo Scientific) for confirmation of acceptable 260/280 nm absorbance ratio as well as determining sample concentrations. Subsequent first-strand cDNA synthesis was done using approximately 1µg of total RNA with Superscript II Reverse Transcriptase and random hexamer primers (Invitrogen) following the company protocol.

Quantitative RT-PCR

Expression levels were assessed using TaqMan Gene Expression Assays. Further details are available at Supplementary Material and Methods.

Rapid Amplification of cDNA Ends (RACE)

We have acquired and used stomach and spleen FirstChoice[®] RLM-RACE Kit (Ambion) according to manufacturer's instructions. Briefly, we have submitted RACE ready cDNA to a first round of amplification using a 5' RACE outer primer and an outer exon 4 *CDH1* primer, followed by a second round using another set of primers. Products were cloned and sequenced. More details are available at Supplementary Material and Methods. All sequences thus obtained were analysed and compiled: the spleen FirstChoice[®] RLM-RACE Kit revealed 6 distinct types of sequences, 2 of which were very similar hence summed in one (*seq4*); the stomach FirstChoice[®] RLM-RACE Kit revealed 8 distinct types of sequences. Data on the coordinates of each sequence (after performing Blast analysis against the human genome (54) is presented on Supplementary Table 1.

Quantitative-SnapShot (Q-SNapShot)

CDH1a quantification was performed by Q-SnapShot (10). Further details on Supplementary Material and Methods.

Primer walking PCR

This strategy was used to characterize the full sequence of transcripts studied. The primers used for the sequential amplification steps are available upon request.

Plasmids construction and virus production

The human E-cadherin nucleotide sequence as reported in the literature (2), was cut from the pcDNA3 plasmid described earlier (61) and cloned into a pLenti6/V5 Directional TOPO® (Invitrogen) giving rise

to the *CDH1* expression vector. The sequence of exons 1 and 2 was later replaced by exon 1a. These vectors, along with the empty vector were used to transduce CHO cells. Viruses were produced following the company instructions. pIRES vectors were subsequently constructed using the above mentioned inserts. Further details are available at Supplementary Material and Methods.

Cell culture, transduction, brefeldin-A and MG132 treatment

CHO and MKN28 cells were grown using standard conditions. These conditions as well as the brefeldin-A and MG132 treatments are described in detail at Supplementary Material and Methods.

Cell sorting and flow cytometry

Stable CHO and MKN28 cells were sorted in a Coulter Epics XL-MCL flow cytometer (Beckman Coulter) using the anti-E-cadherin HECD1 (Zymed Laboratories) and endogenous GFP expression, respectively, in order to obtain a homogeneous population of expressing cells. GFP flow cytometry was performed for MKN28 cells to monitor transfection levels across the course of experiments. Detailed protocol available at Supplementary Material and Methods.

Antibodies, immunofluorescence, immunohistochemistry and microscopy

Antibodies and detailed conditions are available at Supplementary Material and Methods.

Slow aggregation assay and matrigel invasion assay

Cell aggregation assays were performed by coating the wells of a 96-well-plate with 50μ L of an agar solution with subsequent cell seeding. Aggregation was evaluated at 24, 48 and 72hr under an inverted microscope.

For CHO and MKN28 cells invasion assays, Matrigel invasion chambers (BD Biosciences) were used according to the manufacturer conditions. Details are available at Supplementary Material and Methods.

SDS-PAGE, western blotting and immunoprecipitation

Total protein lysates have been used for all experiments. Standard conditions have been employed as described in detail in the Supplementary Material and Methods.

Proteomic analysis

After E-cadherin enrichment by immunoprecipitation, proteins were separated by SDS-PAGE using 3µg of total protein. Following SDS-PAGE separation, proteins were stained, excised and MS and MS/MS peptide mass spectra were acquired with a MALDI-TOF/TOF 4700 Proteomics Analyzer. Detailed description is available at Supplementary Material and Methods.

Chicken embryo in vivo angiogenesis assay

The chicken embryo chorioallantoic membrane (CAM) model was used to evaluate angiogenic response of MKN28 parental and engineered cell lines. The number of new vessels growing radially towards the ring area was counted in a blind fashion. Further details are available at Supplementary Material and Methods.

CDH1a siRNA treatment

A custom *CDH1a* specific siRNA was designed (IDT). Briefly, cells were seeded into 6-well plates and grown in standard conditions until transfection with 100nM of CDH1a siRNA with Lipofectamin 2000 following manufacturer's instructions. After 60hrs we proceeded to invasion assays as described earlier. Remaining cells were used for RNA extraction, *CDH1a*, *IFITM1* and *IFI27* quantification by real-time PCR. A non-silencing siRNA (ThermoScientific) was used as negative control.

Gene expression array

Biotinylated cRNA targets were synthesized from each sample and hybridized to Affymetrix oligonucleotide chips according to manufacturers' instruction (Affymetrix Inc.). GeneChips® Human Genome U133 Plus 2.0 containing 54.000 probe sets (47,000 transcripts and variants including 38,500

well-characterized human genes) were used. The data discussed in this publication have been deposited in NCBI's Gene Expression Omnibus (62) and are accessible through GEO Series accession number GSE32540 (http://www.ncbi.nlm.nih.gov/geo/query/acc.cgi?acc=GSE32540). Details concerning the analysis of data are available at Supplementary Material and Methods.

Statistical analysis

R statistical program was used for the construction of standard boxplots, plotted with whiskers and outliers calculated with a maximum of 1.5 IQR. Due to the non-normal distribution of the data, a non-parametric test, in particular the Wilcoxon Rank Sum Test was used to calculate significance. The *P*-values obtained were further corrected by using the Bonferroni Correction due to the multiple testing performed. Corrected *P*-values <0.05 were considered statistically significant.

Funding

The work was supported by The Portuguese Foundation for Science and Technology (FCT) [Projects: PTDC/SAU-GMG/72168/2006; FCOMP-01-0124-FEDER-015779 (Ref. FCT PTDC/SAU-GMG/110785/2009); PhD grants: SFRH/BD/41223/2007 to HP, SFRH/BD/46462/2008 to RC, SFRH/BD/44074/2008 to JC, SFRH/BD/32984/2006 to PO]. Salary support to CO from POPH – QREN/Type 4.2, European Social Fund and Portuguese Ministry of Science and Technology (MCTES); HP was a recipient of an EMBO short-term fellowship ASTF 239.00-2010.

Acknowledgments

The authors acknowledge Paula Silva and Adriana Rocha, Bárbara Gomes and Professor Fátima Carneiro for the support provided with tissue processing, immunohistochemistry and analysis immunohistochemistry experiments, respectively. The authors thank Beatriz Carvalho and Nicole van Grieken for the frozen normal spleen samples provided.

The authors declare no conflicts of interest.

References

1 Tsanou, E., Peschos, D., Batistatou, A., Charalabopoulos, A. and Charalabopoulos, K. (2008) The E-cadherin adhesion molecule and colorectal cancer. A global literature approach. *Anticancer research*, **28**, 3815-3826.

2 Berx, G., Staes, K., van Hengel, J., Molemans, F., Bussemakers, M.J., van Bokhoven, A. and van Roy, F. (1995) Cloning and characterization of the human invasion suppressor gene E-cadherin (CDH1). *Genomics*, **26**, 281-289.

3 Frixen, U.H., Behrens, J., Sachs, M., Eberle, G., Voss, B., Warda, A., Lochner, D. and Birchmeier, W. (1991) E-cadherin-mediated cell-cell adhesion prevents invasiveness of human carcinoma cells. *J Cell Biol*, **113**, 173-185.

4 Vleminckx, K., Vakaet, L., Jr., Mareel, M., Fiers, W. and van Roy, F. (1991) Genetic manipulation of E-cadherin expression by epithelial tumor cells reveals an invasion suppressor role. *Cell*, **66**, 107-119.

5 Van Aken, E., De Wever, O., Correia da Rocha, A.S. and Mareel, M. (2001) Defective Ecadherin/catenin complexes in human cancer. *Virchows Archiv : an international journal of pathology*, **439**, 725-751.

6 Karam, R., Carvalho, J., Bruno, I., Graziadio, C., Senz, J., Huntsman, D., Carneiro, F., Seruca, R., Wilkinson, M.F. and Oliveira, C. (2008) The NMD mRNA surveillance pathway downregulates aberrant E-cadherin transcripts in gastric cancer cells and in CDH1 mutation carriers. *Oncogene*, **27**, 4255-4260.

7 Onder, T.T., Gupta, P.B., Mani, S.A., Yang, J., Lander, E.S. and Weinberg, R.A. (2008) Loss of Ecadherin promotes metastasis via multiple downstream transcriptional pathways. *Cancer Res*, **68**, 3645-3654.

8 Simoes-Correia, J., Figueiredo, J., Oliveira, C., van Hengel, J., Seruca, R., van Roy, F. and Suriano, G. (2008) Endoplasmic reticulum quality control: a new mechanism of E-cadherin regulation and its implication in cancer. *Hum Mol Genet*, **17**, 3566-3576.

9 Oliveira, C., Senz, J., Kaurah, P., Pinheiro, H., Sanges, R., Haegert, A., Corso, G., Schouten, J., Fitzgerald, R., Vogelsang, H. *et al.* (2009) Germline CDH1 deletions in hereditary diffuse gastric cancer families. *Hum Mol Genet*, **18**, 1545-1555.

10 Pinheiro, H., Bordeira-Carrico, R., Seixas, S., Carvalho, J., Senz, J., Oliveira, P., Inacio, P., Gusmao, L., Rocha, J., Huntsman, D. *et al.* (2010) Allele-specific CDH1 downregulation and hereditary diffuse gastric cancer. *Hum Mol Genet*, **19**, 943-952.

Peinado, H., Olmeda, D. and Cano, A. (2007) Snail, Zeb and bHLH factors in tumour progression: an alliance against the epithelial phenotype? *Nat Rev Cancer*, **7**, 415-428.

12 Oda, T., Kanai, Y., Oyama, T., Yoshiura, K., Shimoyama, Y., Birchmeier, W., Sugimura, T. and Hirohashi, S. (1994) E-cadherin gene mutations in human gastric carcinoma cell lines. *Proc Natl Acad Sci U S A*, **91**, 1858-1862.

Oliveira, C., Sousa, S., Pinheiro, H., Karam, R., Bordeira-Carrico, R., Senz, J., Kaurah, P., Carvalho, J., Pereira, R., Gusmao, L. *et al.* (2009) Quantification of epigenetic and genetic 2nd hits in CDH1 during hereditary diffuse gastric cancer syndrome progression. *Gastroenterology*, **136**, 2137-2148.

Guilford, P., Hopkins, J., Harraway, J., McLeod, M., McLeod, N., Harawira, P., Taite, H., Scoular, R., Miller, A. and Reeve, A.E. (1998) E-cadherin germline mutations in familial gastric cancer. *Nature*, **392**, 402-405.

15 Carvalho, J., van Grieken, N.C., Pereira, P.M., Sousa, S., Tijssen, M., Buffart, T.E., Diosdado, B., Grabsch, H., Santos, M.A.S., Meijer, G. *et al.* (2012) Lack of microRNA-101 causes E-cadherin functional deregulation through EZH2 upregulation in intestinal gastric cancer. *Journal of Pathology*.

Stemmler, M.P., Hecht, A., Kinzel, B. and Kemler, R. (2003) Analysis of regulatory elements of Ecadherin with reporter gene constructs in transgenic mouse embryos. *Dev Dyn*, **227**, 238-245. 17 Stemmler, M.P., Hecht, A. and Kemler, R. (2005) E-cadherin intron 2 contains cis-regulatory elements essential for gene expression. *Development*, **132**, 965-976.

18 Oliveira, P., Sanges, R., Huntsman, D., Stupka, E. and Oliveira, C. (2012) Characterization of the intronic portion of cadherin superfamily members, common cancer orchestrators. *European journal of human genetics : EJHG*.

19 Nilsen, T.W. and Graveley, B.R. (2010) Expansion of the eukaryotic proteome by alternative splicing. *Nature*, **463**, 457-463.

20 Pan, Q., Shai, O., Lee, L.J., Frey, B.J. and Blencowe, B.J. (2008) Deep surveying of alternative splicing complexity in the human transcriptome by high-throughput sequencing. *Nat Genet*, **40**, 1413-1415.

21 Wang, E.T., Sandberg, R., Luo, S., Khrebtukova, I., Zhang, L., Mayr, C., Kingsmore, S.F., Schroth, G.P. and Burge, C.B. (2008) Alternative isoform regulation in human tissue transcriptomes. *Nature*, **456**, 470-476.

Yu, W., Gius, D., Onyango, P., Muldoon-Jacobs, K., Karp, J., Feinberg, A.P. and Cui, H. (2008) Epigenetic silencing of tumour suppressor gene p15 by its antisense RNA. *Nature*, **451**, 202-206.

Bates, D.O., Cui, T.G., Doughty, J.M., Winkler, M., Sugiono, M., Shields, J.D., Peat, D., Gillatt, D. and Harper, S.J. (2002) VEGF165b, an inhibitory splice variant of vascular endothelial growth factor, is down-regulated in renal cell carcinoma. *Cancer Res*, **62**, 4123-4131.

Brauer, P.M., Zheng, Y., Evans, M.D., Dominguez-Brauer, C., Peehl, D.M. and Tyner, A.L. (2011) The alternative splice variant of protein tyrosine kinase 6 negatively regulates growth and enhances PTK6-mediated inhibition of beta-catenin. *PloS one*, **6**, e14789.

25 Crawford, G.E., Holt, I.E., Whittle, J., Webb, B.D., Tai, D., Davis, S., Margulies, E.H., Chen, Y., Bernat, J.A., Ginsburg, D. *et al.* (2006) Genome-wide mapping of DNase hypersensitive sites using massively parallel signature sequencing (MPSS). *Genome research*, **16**, 123-131.

Sorek, R., Ast, G. and Graur, D. (2002) Alu-containing exons are alternatively spliced. *Genome research*, **12**, 1060-1067.

27 Davydov, E.V., Goode, D.L., Sirota, M., Cooper, G.M., Sidow, A. and Batzoglou, S. (2010) Identifying a high fraction of the human genome to be under selective constraint using GERP++. *PLoS computational biology*, **6**, e1001025.

Takatsuki, A. and Tamura, G. (1985) [Inhibitors affecting synthesis and intracellular translocation of glycoproteins as probes]. *Tanpakushitsu kakusan koso. Protein, nucleic acid, enzyme*, **30**, 417-440.

29 Ribatti, D., Vacca, A., Roncali, L. and Dammacco, F. (2000) The chick embryo chorioallantoic membrane as a model for in vivo research on anti-angiogenesis. *Current pharmaceutical biotechnology*, **1**, 73-82.

30 Ribatti, D., Nico, B., Vacca, A., Roncali, L., Burri, P.H. and Djonov, V. (2001) Chorioallantoic membrane capillary bed: a useful target for studying angiogenesis and anti-angiogenesis in vivo. *The Anatomical record*, **264**, 317-324.

Tufan, A.C. and Satiroglu-Tufan, N.L. (2005) The chick embryo chorioallantoic membrane as a model system for the study of tumor angiogenesis, invasion and development of anti-angiogenic agents. *Current cancer drug targets*, **5**, 249-266.

Perl, A.K., Wilgenbus, P., Dahl, U., Semb, H. and Christofori, G. (1998) A causal role for Ecadherin in the transition from adenoma to carcinoma. *Nature*, **392**, 190-193.

33 Xie, X., Mikkelsen, T.S., Gnirke, A., Lindblad-Toh, K., Kellis, M. and Lander, E.S. (2007) Systematic discovery of regulatory motifs in conserved regions of the human genome, including thousands of CTCF insulator sites. *Proc Natl Acad Sci U S A*, **104**, 7145-7150.

34 Kim, T.H., Abdullaev, Z.K., Smith, A.D., Ching, K.A., Loukinov, D.I., Green, R.D., Zhang, M.Q., Lobanenkov, V.V. and Ren, B. (2007) Analysis of the vertebrate insulator protein CTCF-binding sites in the human genome. *Cell*, **128**, 1231-1245.

Lander, E.S., Linton, L.M., Birren, B., Nusbaum, C., Zody, M.C., Baldwin, J., Devon, K., Dewar, K., Doyle, M., FitzHugh, W. *et al.* (2001) Initial sequencing and analysis of the human genome. *Nature*, **409**, 860-921.

Lev-Maor, G., Sorek, R., Shomron, N. and Ast, G. (2003) The birth of an alternatively spliced exon: 3' splice-site selection in Alu exons. *Science*, **300**, 1288-1291.

37 Chen, L.L., DeCerbo, J.N. and Carmichael, G.G. (2008) Alu element-mediated gene silencing. *EMBO J*, **27**, 1694-1705.

38 Stephen, S., Pheasant, M., Makunin, I.V. and Mattick, J.S. (2008) Large-scale appearance of ultraconserved elements in tetrapod genomes and slowdown of the molecular clock. *Molecular biology and evolution*, **25**, 402-408.

Ribeiro, A.S., Albergaria, A., Sousa, B., Correia, A.L., Bracke, M., Seruca, R., Schmitt, F.C. and Paredes, J. (2010) Extracellular cleavage and shedding of P-cadherin: a mechanism underlying the invasive behaviour of breast cancer cells. *Oncogene*, **29**, 392-402.

40 Ahner, A. and Brodsky, J.L. (2004) Checkpoints in ER-associated degradation: excuse me, which way to the proteasome? *Trends Cell Biol*, **14**, 474-478.

41 Yoshida, H. (2007) ER stress and diseases. *The FEBS journal*, **274**, 630-658.

42 Yang, Y., Lee, J.H., Kim, K.Y., Song, H.K., Kim, J.K., Yoon, S.R., Cho, D., Song, K.S., Lee, Y.H. and Choi, I. (2005) The interferon-inducible 9-27 gene modulates the susceptibility to natural killer cells and the invasiveness of gastric cancer cells. *Cancer letters*, **221**, 191-200.

43 Hatano, H., Kudo, Y., Ogawa, I., Tsunematsu, T., Kikuchi, A., Abiko, Y. and Takata, T. (2008) IFNinduced transmembrane protein 1 promotes invasion at early stage of head and neck cancer progression. *Clinical cancer research : an official journal of the American Association for Cancer Research*, **14**, 6097-6105.

44 Yu, F., Ng, S.S., Chow, B.K., Sze, J., Lu, G., Poon, W.S., Kung, H.F. and Lin, M.C. (2011) Knockdown of interferon-induced transmembrane protein 1 (IFITM1) inhibits proliferation, migration, and invasion of glioma cells. *Journal of neuro-oncology*, **103**, 187-195.

45 Rasmussen, U.B., Wolf, C., Mattei, M.G., Chenard, M.P., Bellocq, J.P., Chambon, P., Rio, M.C. and Basset, P. (1993) Identification of a new interferon-alpha-inducible gene (p27) on human chromosome 14q32 and its expression in breast carcinoma. *Cancer Res*, **53**, 4096-4101.

46 Suomela, S., Cao, L., Bowcock, A. and Saarialho-Kere, U. (2004) Interferon alpha-inducible protein 27 (IFI27) is upregulated in psoriatic skin and certain epithelial cancers. *The Journal of investigative dermatology*, **122**, 717-721.

47 Wenzel, J., Tomiuk, S., Zahn, S., Kusters, D., Vahsen, A., Wiechert, A., Mikus, S., Birth, M., Scheler, M., von Bubnoff, D. *et al.* (2008) Transcriptional profiling identifies an interferon-associated host immune response in invasive squamous cell carcinoma of the skin. *International journal of cancer. Journal international du cancer*, **123**, 2605-2615.

Bierie, B. and Moses, H.L. (2006) TGF-beta and cancer. *Cytokine & growth factor reviews*, **17**, 29-40.

49 Akhurst, R.J. and Derynck, R. (2001) TGF-beta signaling in cancer--a double-edged sword. *Trends Cell Biol*, **11**, S44-51.

50 Guasch, G., Schober, M., Pasolli, H.A., Conn, E.B., Polak, L. and Fuchs, E. (2007) Loss of TGFbeta signaling destabilizes homeostasis and promotes squamous cell carcinomas in stratified epithelia. *Cancer cell*, **12**, 313-327.

51 Ma, L., Pang, C.N., Li, S.S. and Wilkins, M.R. (2010) Proteins deleterious on overexpression are associated with high intrinsic disorder, specific interaction domains, and low abundance. *Journal of proteome research*, **9**, 1218-1225.

52 Gsponer, J., Futschik, M.E., Teichmann, S.A. and Babu, M.M. (2008) Tight regulation of unstructured proteins: from transcript synthesis to protein degradation. *Science*, **322**, 1365-1368.

53 Doherty, M.K., Hammond, D.E., Clague, M.J., Gaskell, S.J. and Beynon, R.J. (2009) Turnover of the human proteome: determination of protein intracellular stability by dynamic SILAC. *Journal of proteome research*, **8**, 104-112.

54 Flicek, P., Aken, B.L., Ballester, B., Beal, K., Bragin, E., Brent, S., Chen, Y., Clapham, P., Coates, G., Fairley, S. *et al.* (2010) Ensembl's 10th year. *Nucleic Acids Res*, **38**, D557-562.

55 Davuluri, R.V., Grosse, I. and Zhang, M.Q. (2001) Computational identification of promoters and first exons in the human genome. *Nat Genet*, **29**, 412-417.

Jurka, J., Kapitonov, V.V., Pavlicek, A., Klonowski, P., Kohany, O. and Walichiewicz, J. (2005) Repbase Update, a database of eukaryotic repetitive elements. *Cytogenetic and genome research*, **110**, 462-467.

57 Boguski, M.S., Lowe, T.M. and Tolstoshev, C.M. (1993) dbEST--database for "expressed sequence tags". *Nat Genet*, **4**, 332-333.

58 Rhead, B., Karolchik, D., Kuhn, R.M., Hinrichs, A.S., Zweig, A.S., Fujita, P.A., Diekhans, M., Smith, K.E., Rosenbloom, K.R., Raney, B.J. *et al.* (2010) The UCSC Genome Browser database: update 2010. *Nucleic Acids Res*, **38**, D613-619.

59 Birney, E., Stamatoyannopoulos, J.A., Dutta, A., Guigo, R., Gingeras, T.R., Margulies, E.H., Weng, Z., Snyder, M., Dermitzakis, E.T., Thurman, R.E. *et al.* (2007) Identification and analysis of functional elements in 1% of the human genome by the ENCODE pilot project. *Nature*, **447**, 799-816.

Kodzius, R., Kojima, M., Nishiyori, H., Nakamura, M., Fukuda, S., Tagami, M., Sasaki, D., Imamura, K., Kai, C., Harbers, M. *et al.* (2006) CAGE: cap analysis of gene expression. *Nature methods*, **3**, 211-222.

Suriano, G., Oliveira, C., Ferreira, P., Machado, J.C., Bordin, M.C., De Wever, O., Bruyneel, E.A., Moguilevsky, N., Grehan, N., Porter, T.R. *et al.* (2003) Identification of CDH1 germline missense mutations associated with functional inactivation of the E-cadherin protein in young gastric cancer probands. *Hum Mol Genet*, **12**, 575-582.

62 Edgar, R., Domrachev, M. and Lash, A.E. (2002) Gene Expression Omnibus: NCBI gene expression and hybridization array data repository. *Nucleic Acids Res*, **30**, 207-210.

Legends to figures

Figure 1. *CDH1* **qRT-PCR expression ratio using two probes targeting different gene regions,** exon **6/7 and exon 1/2 boundaries.** Normal tissues were tested and all presented higher expression levels with the downstream probe indicating the existence of transcripts encompassing exons 6-7 but excluding exons 1-2

Figure 2. CDH1 *gene locus gives rise to several transcripts in addition to the canonic.* A. *CDH1** indicates the canonical transcript and *CDH1*[§] designates the novel transcripts herein described. *ESTs* are the Expressed Sequence Tags deposited in the dbEST database for *CDH1* gene. Genomic elements represent the features annotated for this genome location: *CpG* indicates the existence of a CpG island; *EF* is the site where the first exon of a given transcript is predicted to be located; *AluSc* signifies the existence of a Alu repeat from the Sc subcategory in the region; *DNaseI* represents DNase I hypersensitive sites detected by ChIP-Seq and; *CTCF* means the prediction of a CCCTC-binding factor (CTCF) binding site. Zoom in pictures of shaded areas I and II are represented in the lower panel. B. *RACE (spleen)* and *RACE (stomach)* describe the sequences that resulted from our Rapid Amplification of cDNA Ends experiments and are depicted in the pie charts that summarize the results obtained.

Figure 3. CDH1a *is highly expressed in normal spleen and is detected with an anti-E-cadherin antibody.* A. Q-SnapShot expression of *CDH1a* transcript in normal tissues. Spleen has the highest level of *CDH1a* expression and stomach presents no expression. B and C. Immunohistochemistry performed with an anti-E-cadherin antibody targeting a common region between *CDH1a* and the canonic transcript in sections of normal paraffin embedded spleen and stomach tissues. B. In spleen, a non-epithelial tissue (without canonic E-cadherin expression), the antibody stains unidentified globular structures formed by small groups of cells. C. Gastric epithelial expression displays the expected pattern with the staining at the basolateral surface of adjacent cells. Scale bars: upper panel - 200 μ m and lower panel – 100 μ m.

Figure 4. CDH1a is translated, in vitro, into an E-cadherin isoform that interacts with β - and p120 catenins at the membrane of CHO (E-cadherin-negative) cells and elicits cell aggregation and invasion suppression. A. Schematic representation of the canonic protein and from the putative CDH1a isoform. In dark and light grey areas are the specific regions from both proteins, respectively. The white corresponds to the common part that is predicted to be cleaved during protein processing that occurs at the site marked by a grey line. The black area corresponds to the expected mature proteins and the asterisk marks the epitope recognized by the antibody used. B. CDH1a mature protein has a similar size to the canonic Ecadherin. C. CDH1a immature form is, as expected, smaller than the canonic protein as exons 1 and 2 are replaced by exon 1a. D. CDH1a is able to bind to β-catenin and p120ctn, components of the adhesion complex as happens with the canonic E-cadherin protein. E. Coomassie blue stained gel showing Ecadherin and CDH1a processed and unprocessed bands. F and G. CDH1a isoform recruits and colocalizes with β -catenin and p120ctn at the cell membrane as occurs for E-cadherin. No staining is observed for mock transfected cells. Scale bar – 15 µm. H. CDH1a isoform is able to elicit cell-cell aggregation as for E-cadherin, in contrast to the empty vector (mock) transduced cells. Scale bar -200μm. I. CDH1a confers statistically significant strong invasion suppression capacity as the canonic protein when compared to mock cells (P=.026 and .019, respectively).

Figure 5. *CDH1a overexpression in E-cadherin expressing MKN28 cells does not interfere with canonic protein localization*. A. Flow cytometry was performed to monitor MKN28 transfection efficiencies of pIRES_*E-cadherin*, Mock and *CDH1a* constructs. B. GFP fluorescence levels of MKN28 *E-cadherin*, Mock and *CDH1a* cells. Scale bar – 15 μ m. C. E-cadherin immunofluorescence of MKN28 *E-cadherin*, Mock and *CDH1a* cells. Overexpression of the transcripts has not influenced normal membrane protein localization. Scale bar – 15 μ m. D. QRT-PCR levels with two assays targeting different regions, 1-2 and 6-7 *CDH1* exon boundaries. As expected, *CDH1* overexpression results in higher levels of expression for both probes while for *CDH1a* only the second assay detects increased transcription levels. E. E-cadherin Western blot reveals an equivalent level of protein expression in each

cell line. F. E-cadherin Western blot of MG132 treated cells shows that transfection results in an effective increase in protein translation that is masked by proteasome degradation.

Figure 6. *CDH1a overexpression promotes mild MKN28 (E-cadherin positive cells) aggregation and increases invasion and angiogenesis levels.* A. Slow aggregation assay showing that MKN28 *E-cadherin* cells aggregate more compactly than mock cells, as expected. Interestingly, *CDH1a* cells present intermediate compaction. Scale bar – 3 mm. B. Invasion assay demonstrates significantly higher levels in MKN28 *CDH1a* in comparison both to MKN28 Mock and *CDH1* cells. C. CAM angiogenesis assay shows an increase in blood vessels formation between MKN28 Mock and MKN28 *CDH1* cells. *CDH1a* led to a significant increase in angiogenesis when compared to Mock cells. D. CAM angiogenesis assay images showing the ring used for cell inoculation, the tumor formed and blood vessels nurturing the tumor. Scale bar – 1 mm. E. Pan-cytokeratin immunohistochemistry of a CAM section showing the chorion (ch) and the allantoic (al) sides of the membrane. Scale bar – 400 μ m.

Figure 7. CDH1a overexpression in MKN28 cells increases *IFITM1* and *IFI27* levels. A and B. MKN28 CDH1a overexpressing cells display significant IFITM1 and IFI27 gene expression upregulation when compared to controls.

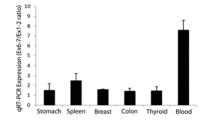
Figure 8. Invasion, IFITM1 and IFI27 levels are reduced upon CDH1a specific downregulation. A. MKN28 CDH1a overexpressing cells were treated with a specific siRNA leading to 35% of knockdown when compared to the non-silencing siRNA. B. Invasion levels were reduced in 73% after siRNA treatment. C. IFITM1 and IFI27 levels were also reduced by 31% and 45%, respectively.

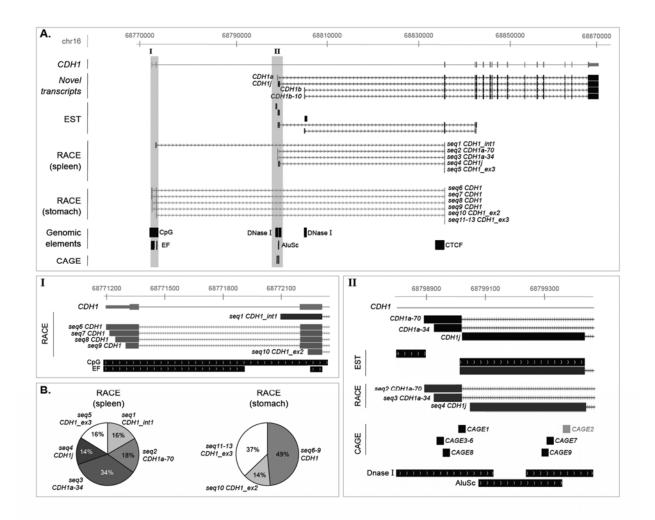
Figure 9. *CDH1a transcript is overexpressed in gastric cancer cell lines.* A. Stomach qRT-PCR expression of *CDH1 and CDH1a* transcripts. Cell lines present high expression heterogeneity when compared with stomach values, although the majority express lower *CDH1* levels than the normal tissue. B. Q-SNapShot *CDH1a* expression levels show that this transcript is completely absent in normal stomach but *de novo* in most of the gastric cell lines tested.

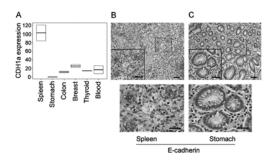
Figure 10. CDH1a effect model in gastric cancer cell lines. In normal stomach only E-cadherin is expressed from the CDH1 locus. This protein is expressed at the cell membrane where it exerts its main function being responsible for cell-cell adhesion. In gastric cancer cell lines CDH1a isoform is produced from the CDH1 locus. This isoform is expressed at the cell membrane where it impairs normal E-cadherin function as seen by adhesion and invasion assays. Gene expression array and qRT-PCR revealed IFITM1 and IFI27 mRNA upregulation. Moreover, in CAM assay, angiogenesis is induced upon CDH1a overexpression.

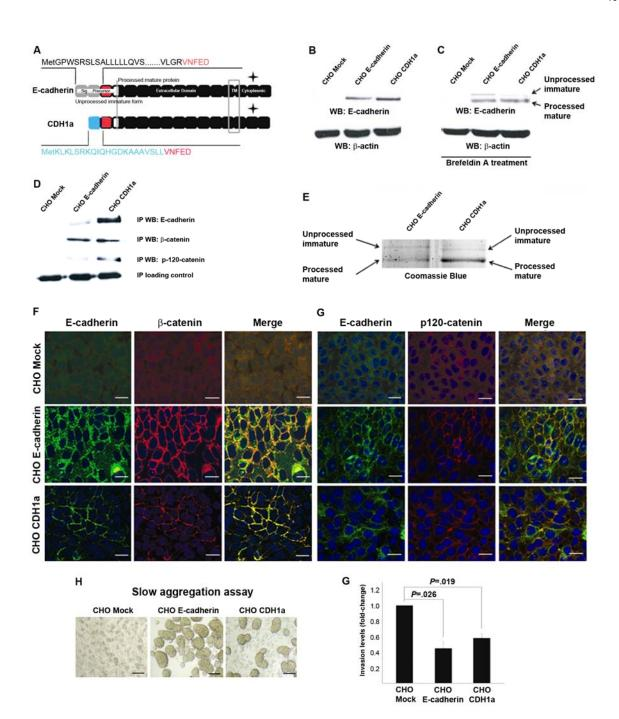
Abbreviations: HDGC, Hereditary Diffuse Gastric Cancer; DGC, Diffuse Gastric Cancer; GC, Gastric Cancer; PBLs, Peripheral Blood Lymphocytes.

Grant support: Supported by The Portuguese Foundation for Science and Technology (FCT) (Projects: PTDC/SAU-GMG/72168/2006; FCOMP-01-0124-FEDER-015779 (Ref. FCT PTDC/SAU-GMG/110785/2009); PhD grants: SFRH/BD/41223/2007-HP, SFRH/BD/46462/2008-RC, SFRH/BD/44074/2008-JC, SFRH/BD/32984/2006-PO; salary support to CO from POPH – QREN/Type 4.2, European Social Fund and Portuguese Ministry of Science and Technology (MCTES)). IPATIMUP is an Associate Laboratory of the Portuguese Ministry of Science, Technology and Higher Education and is partially supported by FCT. HP was a recipient of an EMBO short-term fellowship ASTF 239.00-2010.

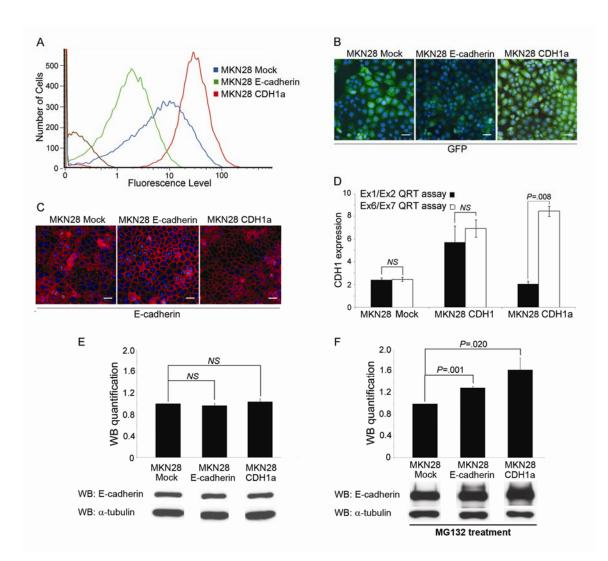


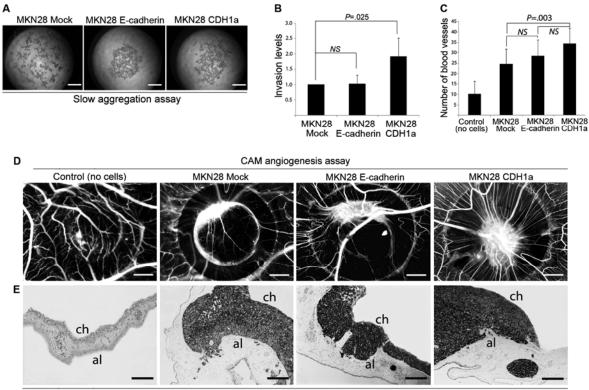






Downloaded from http://hmg.oxfordjournals.org/ at INSERM on July 4, 2012





Pan cytokeratin

